# CHIPSIM: A Co-Simulation Framework for Deep Learning on Chiplet-Based Systems

Lukas Pfromm\*, Alish Kanani\*, Harsh Sharma<sup>†</sup>, Janardhan Rao Doppa<sup>†</sup>, Partha Pratim Pande<sup>†</sup>, Umit Y. Ogras\*

\*University of Wisconsin–Madison, Madison, WI, USA, <sup>†</sup>Washington State University, Pullman, WA, USA

Abstract— Due to reduced manufacturing yields, traditional monolithic chips cannot keep up with the compute, memory, and communication demands of data-intensive applications, such as rapidly growing deep neural network (DNN) models. Chipletbased architectures offer a cost-effective and scalable solution by integrating smaller chiplets via a network-on-interposer (NoI). Fast and accurate simulation approaches are critical to unlocking this potential, but existing methods lack the required accuracy, speed, and flexibility. To address this need, this work presents CHIPSIM, a comprehensive co-simulation framework designed for parallel DNN execution on chiplet-based systems. CHIPSIM concurrently models computation and communication, accurately capturing network contention and pipelining effects that conventional simulators overlook. Furthermore, it profiles the chiplet and NoI power consumptions at microsecond granularity for precise transient thermal analysis. Extensive evaluations with homogeneous/heterogeneous chiplets and different NoI architectures demonstrate the framework's versatility, up to 340% accuracy improvement, and power/thermal analysis capability.

Index Terms—Chiplets, Heterogeneous integration, Cosimulation, Deep neural networks (DNNs), Thermal modeling

#### I. INTRODUCTION

Deep neural networks (DNNs) require increasingly powerful systems due to their growing size and computational demands [1]. Traditional monolithic 2D chips have grown substantially to keep up with the exponential increase in model parameters and processing requirements. However, monolithic chips becomes less economical to manufacture due to declining yield as chip size increases [2]. These trends have driven a new advanced packaging and heterogeneous integration approach using smaller dies called chiplets [3, 4].

Chiplet-based systems integrate many chiplets into a single package, as illustrated in Figure 1. Each chiplet has a lower manufacturing cost than a monolithic chip due to its small size and higher yield [3, 5]. Combining chiplets into a single package can deliver higher performance and energy efficiency than monolithic systems at comparable costs. Moreover, the greater modularity and heterogeneity enrich the design space, enabling systems tailored to specific application requirements [6].

Chiplet-based systems have experienced widespread adoption in both academia and industry. Studies in this area have explored various topics, including network topology, packaging, interconnects, power and thermal analysis, and application mapping [7]. In parallel, industry adoption has also accelerated, with notable examples such as NVIDIA's B200 [8], Intel's Agilex and Meteor Lake [9, 10], AMD's Ryzen, EPYC, and Instinct [4], and other commercial products built on chiplet architectures. Federal funding initiatives, like the National Advanced Packaging Manufacturing Program

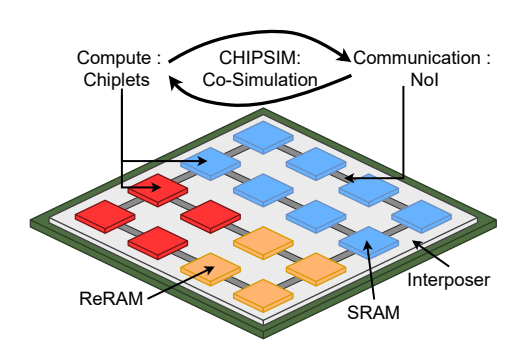


Fig. 1: An illustration of the CHIPSIM framework on a non-mesh heterogeneous chiplet-based system.

(NAPMP) and Scalable Memory Architecture Program, have also been launched to support chiplet-based system development [11, 12]. This convergence of academic research, industrial implementation, and strategic initiatives underscores the importance of chiplets and the supporting tools for their development.

Chiplet-based systems require fast and accurate evaluation methods to quantify the trade-off between competing objectives, such as performance, energy efficiency, and temperature. Simulations are essential throughout the design process, from early exploration and chiplet selection to floorplanning and workload mapping, especially when hardware prototypes are unavailable. Navigating complex and conflicting constraints to meet the design objectives is intractable without reliable tools. Large-scale heterogeneous architectures and target workloads further increase the complexity. As design complexity grows, fast and accurate simulation is key to enabling iteration, guiding decisions, and driving innovation.

Current research on chiplet-based systems relies on simulation methods that are accurate but slow and inflexible or fast but inaccurate, as illustrated in Figure 2. For instance, when cycle-level accuracy is needed, gem5 [13, 14] can simulate the computations, while HeteroGarnet [15] or Booksim [16] simulates communication. However, gem5 is slow and has limited support for alternative processing technologies beyond CMOS designs. To achieve faster simulations or explore novel configurations such as chiplets based on in-memory computing (IMC), researchers frequently combine existing simulators in an ad-hoc fashion. Specifically, the computation and communication phases of the target applications are considered separately, with limited interaction between them [17– 21]. Improvised methods cannot accurately capture complex behaviors like traffic contention and pipelining of DNN model layers, which can impact the simulation performance results by more than 340%, as we demonstrate in Section V. Moreover, decoupling computation and communication prevents a co-

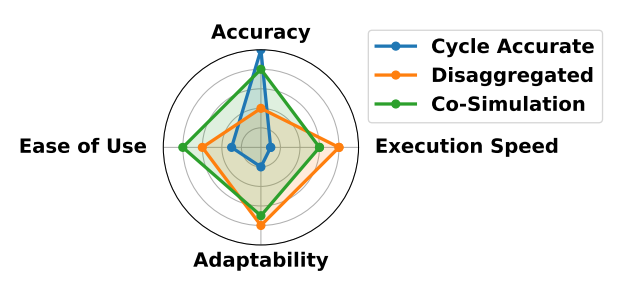


Fig. 2: A visual comparison between existing simulators and the proposed simulation methodology.

herent notion of time, making modeling time-based behavior such as transient power analysis impossible. Thermal analysis, a crucial aspect of chiplet-based systems, requires time-based power consumption. Therefore, chiplet-based systems need fast, accurate, and modular co-simulation approaches.

This paper introduces CHIPSIM, a co-simulation framework for chiplet-based systems executing DNN models. While cosimulation has been explored in other domains, CHIPSIM is the first framework to apply this methodology to chipletbased architectures. In addition to co-simulation, CHIPSIM coordinates computation and communication phases under a unified notion of global simulation time, enabling concurrent execution of multiple DNN models while accurately capturing their interactions and system-level effects. CHIPSIM begins by simulating the first layer of the target DNN workload. Upon completion, it simulates the communication of the resulting activations to the chiplet that will run the consecutive layer. This way, computation and communication events are simulated in tandem while keeping track of the global time. When multiple DNN models arrive in a stream and must execute in parallel on the same system, CHIPSIM orchestrates concurrent computation and communication simulations while accurately capturing their interactions and impacts on each other. For example, the communication simulation at any given time accounts for all active chiplet-to-chiplet data movement of all DNNs in the system to capture network contention accurately. Our results show contention becomes a dominant factor in communication latency, especially during highly utilized times, yet it remains unmodeled by current approaches.

As a critical and novel aspect, CHIPSIM incorporates a detailed power tracking mechanism that generates power and thermal profiles with microsecond-level granularity for every chiplet. These power profiles enable transient and steady-state thermal analysis. Additionally, CHIPSIM supports both heterogeneous chiplet types and custom network-on-interposer (NoI) topologies to support extensive design-space exploration and diverse configurations. Due to its modularity, CHIPSIM can utilize different computation and communication simulators. In this work, we primarily target IMC chiplets simulated using CimLoop [22] and use HeteroGarnet [15] for communication. However, we perform additional hardware validations where CiMLoop is replaced with an analytical compute model. We emphasize that the proposed framework is not limited to any processing technology or choice of simulators.

The key contributions of this work are as follows:

 A comprehensive co-simulation framework that captures the salient features of hardware execution by modeling

- computation and communication events,
- A concrete realization with open-source tools and modular support for heterogeneous chiplets and NoI topologies,
- Comprehensive evaluations with three different system configurations that demonstrate up to 340% higher accuracy and enable transient power/thermal analysis—capabilities not possible with existing approaches.
- Open-sourced code for the created tool available at github.com/LukasPfromm/CHIPSIM.

The rest of the paper is organized as follows. Section II reviews the related work. Section III details our approach to co-simulation, while Section IV presents a concrete realization. Finally, Section V presents the experimental evaluation, and Section VI concludes the paper.

#### II. RELATED WORK

Chiplet-based system design presents many challenges, from optimizing individual chiplets to NoI design and mapping workloads onto these systems. Many studies have leveraged the modularity enabled by chiplet integration to develop both general-purpose and heterogeneous systems tailored to specific domains, such as AI/ML [4, 10, 25–28]. Similarly, the design of the chiplet interconnection network has attracted significant attention due to its importance in minimizing latency and energy cost incurred by data movement [15, 17–19]. To maximize the performance of these systems after their design, recent studies have proposed methods for mapping computation and communication tasks [18, 29] and optimizations such as DNN layer pipelining [29–31].

Solving these design challenges requires fast, flexible, and accurate simulation models to capture the complex interactions inherent to these architectures. They must adapt to diverse aspects of system design, from chiplet composition and interconnection topology to workload mapping and runtime optimizations, while executing quickly enough to enable broad design space exploration. However, existing simulation approaches fall short in one or more of these aspects, limiting their effectiveness in supporting comprehensive analysis.

Studies that focus purely on NoI design sometimes omit computation performance modeling [17, 18, 20, 21, 32] or perform decoupled compute and communication simulation [19, 23, 26]. While simplifying modeling, this approach introduces inaccuracies since compute-communication interactions are abstracted. Table I compares the features supported by several proposed simulators. Gem5 [13, 14], while not created specifically for chiplets, is a cycle-accurate simulator that has been adapted via the HeteroGarnet simulator [15] to model inter-chiplet traffic. While accurate, cycle-accurate simulation comes at the cost of prohibitive runtime. Additionally, there is no native support for thermal modeling or processing approaches such as IMC [33, 34]. SIAM [23] aims to address the need for IMC chiplet simulation by using NeuroSim [35] for processing simulation in combination with Booksim [16] for traffic modeling. However, it does not support heterogeneous systems or thermal analysis and still requires hours for simulation. To mitigate the high simulation times of previous approaches, HISIM [24] utilizes analytical models instead of existing simulators. This allows for a considerable

TABLE I: Feature comparison of simulation frameworks.

Simulator / Analysis Tool	Sim. Time	Thermal Analysis	Parallel Model Execution	Pipeline Support	Network Contention	Heterogeneous Systems	IMC Support
Gem5 [13, 14] + HeteroGarnet [15]	Weeks	Х	✓	✓	✓	✓	Х
SIAM [23]	Hours	×	×	X	$\checkmark$	×	$\checkmark$
HISIM [24]	Seconds	<b>√</b> *	X	X	×	$\checkmark$	$\checkmark$
CHIPSIM (This Work)	Minutes	$\checkmark$	$\checkmark$	$\checkmark$	$\checkmark$	$\checkmark$	✓

simulation time improvement to the order of milliseconds or seconds. Additionally, thermal modeling is implemented along with native support for IMC chiplets. However, rapid analysis comes at the cost of accuracy and features. Thermal analysis is not transient; instead, discrete thermal simulations are performed for each model layer.

Neither SIAM nor HISIM support the modeling of (1) pipelined behavior, where two or more layers of a model execute concurrently, (2) parallel model execution, where two or more models run simultaneously on the same system, or (3) communication contention, which occurs on the NoI. Therefore, they cannot accurately model the scenario where a stream of models is executed in parallel in the same system, a workload commonly applied to chiplet-based systems [4, 18, 29], while cycle-accurate simulations are too slow. To meet this need, we apply co-simulation to the domain of chiplet-based system simulation and create CHIPSIM. We note that co-simulation is an established methodology across multiple domains, including end-to-end networked systems (e.g., SimBricks [36]) and processor–programming model studies (e.g., SST [37]). CHIPSIM builds on this foundation by adapting time-synchronized simulation to the domain of chipletbased systems executing parallel DNN workloads. Unlike prior frameworks, CHIPSIM integrates compute and communication simulators tailored to chiplet architectures, supports multi-instance DNN pipelines, and provides microsecondresolution thermal analysis by tracking energy and execution timelines across chiplets. This domain-specific instantiation enables accurate performance, power, and thermal modeling in emerging heterogeneous chiplet+NoI designs that are not well supported by existing general-purpose simulation infrastructures. Our evaluations in Section V compare CHIPSIM against two baseline approaches: communication simulation only and decoupled computation-communication modeling (like HISIM and SIAM). The results highlight the need for a fast, accurate, and modular co-simulation framework to integrate computation and communication models coherently. CHIPSIM addresses this need as a comprehensive framework for detailed performance, power, and thermal analysis.

# III. CHIPSIM CHIPLET CO-SIMULATION FRAMEWORK

## A. Overview of the Proposed Framework

DNN models follow a layer-wise execution: (1) the computations of the current layer are executed, (2) the generated activations are transmitted to the hardware resources that will execute the subsequent layer. These computation-communication steps are repeated until the entire model is complete. The CHIPSIM framework accurately models these interactions between computation and communication while multiple DNN model instances run in parallel by tracking

the compute and communication phases of each model individually. Additionally, CHIPSIM tracks the occupancy of each chiplet, since the mapping of subsequent DNN model layers depends upon the execution of previous layers. Tracking detailed utilization statistics can also aid workload mapping and architecture optimization techniques.

The building blocks of the CHIPSIM framework and data flow between them are visualized on the left-hand side of Figure 3. There are three primary user inputs: (1) Target DNN workload, (2) Hardware configuration, (3) Mapping function of the input DNN models to the hardware resources.

The core component of CHIPSIM, the Global Manager, takes these inputs and orchestrates the computation and communication co-simulation as shown in Figure 3. The workload comprises a stream of DNN models, which is continuously read and mapped to the target chiplet-based system by the Global Manager. The mapping strategy for DNN layers is determined by the Mapping Function input. The hardware configuration describes the number and type of chiplets, compute capabilities, memory capacities, and the NoI topology. After mapping, the Global Manager invokes the computation and communication simulators to collect power and performance metrics for each DNN model as a function of time. This section provides a conceptual description of the proposed CHIPSIM framework. This concept can be realized with available compute [13, 22, 38] and communication [15, 16, 39, 40] simulators, as described in Section IV.

## B. Input Workload and Mapping

The input workload is a list of DNN models that will run on the target chiplet-based system. The DNN models are represented in a layer-wise format, where each layer is characterized by its parameters, including the number of input and output layers, filter sizes, and stride lengths.

The Global Manager traverses the Model Queue to find the first DNN model that fits the available memory resources in the target hardware. We allow out-of-order execution of the DNN models to maximize chiplet utilization and prevent smaller models from starving when they arrive after a large model. We emphasize that the CHIPSIM co-simulation framework is oblivious to the specific arbitration method.

After retrieving the next DNN model, the Global Manager utilizes the user-provided Mapping Function to allocate each layer of this DNN model to the available resources in the chiplet-based system. Like the arbitration mechanism, the CHIPSIM framework can be used with any mapping function. To maximize generality, CHIPSIM supports layers that may be too big to fit on one chiplet. In this case, the layer is split into multiple segments, with each segment being mapped to an individual chiplet. As the Global Manager

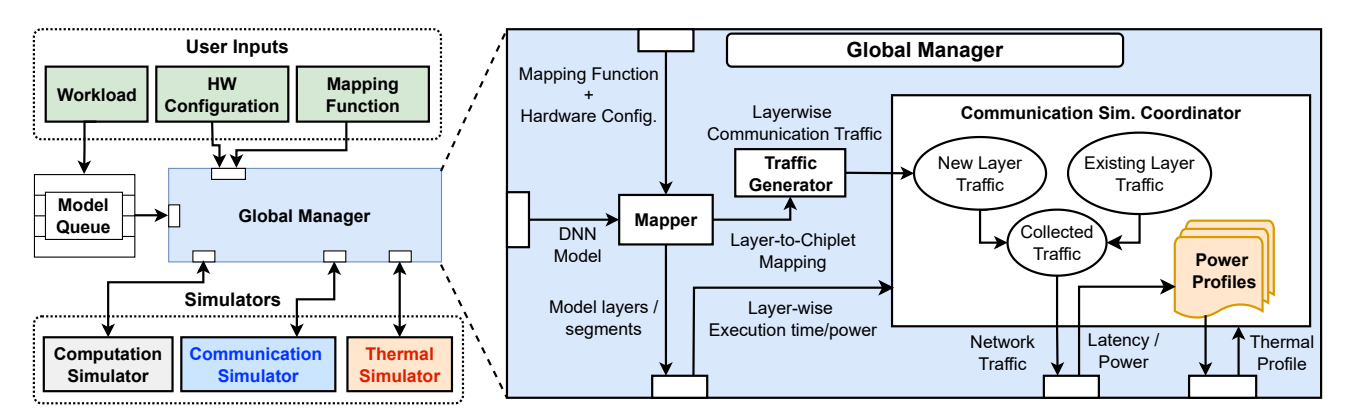


Fig. 3: Outline of the proposed simulation framework.

traverses each layer of the current DNN sequentially, it maps the next layer to a chiplet if there is enough available memory. Otherwise, it divides the layer into the fewest segments that fit the chiplet resources and maps them to minimize the communication cost. Then, it updates the system state to keep track of the memory resource usage in each chiplet. This update ensures that the occupancy of each chiplet is accurate for future DNN mapping operations.

## C. Compute Simulation

Compute operations within each chiplet are independent of the operations executed on other chiplets. To exploit this parallelism, the Global Manager launches a dedicated compute simulation thread for each layer segment mapped to one or more chiplets. Hence, the number of active compute simulator instances equals the number of model segments. Each thread is provided with the physical system configuration—defining chiplet properties such as MAC units, memory hierarchy, and frequency, alongside the DNN layer description (e.g., type, input/output dimensions). The simulator then returns the estimated execution time, energy, and power consumption.

To ensure extensibility and long-term usability, CHIPSIM is designed with a modular interface that decouples the coordinator from specific backends. Each component simulator is invoked independently through a standardized input/output format. For compute simulation, this abstraction allows seamless integration with a range of backends, including analytical models, cycle-accurate simulators, or third-party tools. For example, we replaced the original CiMLoop-based backend with an analytical CPU performance model that estimates compute latency by dividing the number of MAC operations by the sustained throughput (MACs per second) of the target CPU, as shown in Section V-F. Importantly, this substitution requires no modifications to the control flow or data structures of CHIPSIM, demonstrating the generality of the framework. Since simulation progress is decoupled from the internal execution model of each backend, CHIPSIM preserves fidelity while supporting both rapid prototyping and detailed architectural studies.

## D. Communication Simulation

When a compute simulation thread completes, it produces layer-wise compute metrics for that layer as depicted in Figure 3. Layer-wise activations have been previously generated by the traffic generator. The communication simulation is responsible for accurately tracking the communication latency and energy cost. Unlike the computations within each chiplet, the inter-chiplet communication network is a shared resource used by multiple DNN models simultaneously. Hence, there is a single communication simulation thread that accounts for all inter-chiplet communication from all active DNN models. The Global Manager generates the communication traffic for all models and inputs them into a Communication Simulation Coordinator, as shown in Figure 3.

Consider a toy example where the workload consists of only a single DNN model. The Communication Simulation Coordinator would simply dispatch each layer's activation traffic to the network simulator layer by layer. However, since multiple DNN models may run in parallel in a server-class processor, the CHIPSIM framework also handles much more complex cases with tens of concurrent DNN models. To do this, the Communication Simulation Coordinator tracks all other active DNN models and their traffic at a given time. Using the results of the compute simulation operations, the traffic between each chiplet, and the current state of the simulated system, the Communication Simulation Coordinator dispatches communication operations to the network simulator. This coordination allows for the modeling of the contention between layer traffic, as detailed in the following section.

### E. Co-simulation Coordination

We employ an illustrative scenario to describe how CHIP-SIM accurately models the behavior of a chiplet-based system. Scenario description: Three DNN models run in parallel, as shown in a different row along the y-axis in Figure 4. The x-axis shows the simulation time and labels time instances that are important for this discussion. Model A is launched at time 0, while Model B and Model C are launched later with arbitrary offsets, as marked in the figure. For simplicity, Models A and B have three layers, while Model C has two layers. Each model layer alternates between compute and communication phases, corresponding with computing the activations of a given layer and communicating them to the chiplets running the next layer. These phases are shown by black diagonal and light blue plain patterns in Figure 4. Next, we describe the co-simulation behavior step by step using the event diagram.

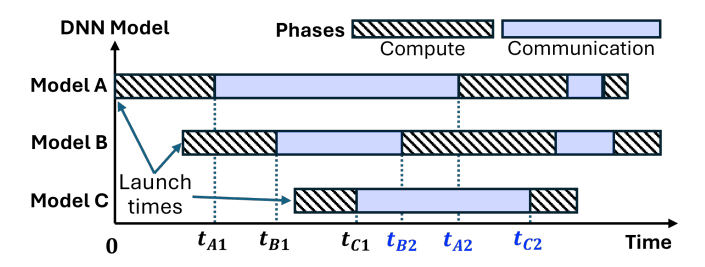


Fig. 4: An illustrative event diagram showing the interleaving of different simulation operations.

**Time**  $0 - t_{A1}$ : At time 0, Model A simulation begins, and after an offset, Model B also starts running. Since no communication simulations are performed until  $t_{A1}$ , there is no data movement (hence no communication simulation) in this interval.

**Time**  $t_{A1} - t_{B1}$ : After Layer-1 of Model A finishes computation at time  $t_{A1}$ , the Global Manager receives the latency and energy for the operation. Additionally, the number of activations between Layer-1 and Layer-2 is known from the Traffic Generator. The chiplets that execute the consecutive layer are known through the Mapping Function. So, the Global Manager generates the network traffic from the chiplet(s) that run Layer-1 (source) to the chiplet(s) that run Laver-2 (destination). Since there is no other active communication during this time, the communication simulation is launched with this traffic. The Global Manager uses the end-to-end communication latency to schedule the computation simulation of Layer-2 of Model A, after the projected communication time passes. Since the first layer of Model B finishes computation at  $t_{B1}$ , i.e., before Model A Layer 1-Layer 2 communication, the communication simulation is updated to account for this overlap, as described next.

**Time**  $t_{B1} - t_{C1}$ : The computation of Layer-1 of Model B finishes at  $t_{B1}$ . As with Model A in the previous time interval, the Global Manager receives the activations produced by the first layer. Then, it generates the network traffic from the chiplet(s) that run Layer-1 to the chiplet(s) that run Layer-2. In contrast to the previous interval, two communication simulations overlap: (1) the remaining portion of Model A Layer 1–2 and (2) Model B Layer 1–2.

Accounting for this overlap is critical to accurately modeling congestion in the inter-chiplet network. Therefore, Global Manager maintains a traffic profile that combines the existing traffic and the new layer traffic created by Layer-1 of Model B. Specifically, it updates the communication simulation to include the remaining part of the existing traffic and the newly generated data. The communication simulation resumes after the combined traffic profile has been created. This communication traffic update process repeats when a compute layer finishes and new activations are present. Similarly, when a certain communication event finishes, this process is paused to get the updated end-to-end communication latency.

**Time**  $t_{C1} - t_{B2}$ : The first compute phase of Model C completes at  $t_{C1}$ . The exact process described for the previous interval is repeated. That is, the Global Manager combines the activations produced by Model C with existing data flows

to generate the updated network traffic. As with Model B, the Global Manager accounts for existing traffic generated by Model A and B. Then, the communication simulation resumes with this combined traffic profile.

Time  $t_{B2}-t_{A2}$  and later:  $t_{B2}$  is the time instance when the Model B Layer 1-Layer 2 communication finishes. So, the Global Manager launches Model B Layer 2 computations at this time. Similarly, Model A communication finishes, and its Layer 2 computation starts at  $t_{A2}$ . The Global Manager repeats the processes described so far continuously until all models and layers are fully executed.

#### IV. CONCRETE METHODOLOGY IMPLEMENTATION

The CHIPSIM framework supports flexible integration of different simulators to match the chiplet communication architectures under study. This section demonstrates a concrete implementation using open-source tools, as shown in Figure 5.

# A. Computation Simulation

Since our experiments focus on IMC chiplets, we adopt CiMLoop [22] as the computation simulator. CiMLoop is selected since it enables modeling a wide range of IMC architectures accurately, with detailed crossbar arrays, peripheral circuits, and analog-digital interfaces, making it well-suited for IMC-based DNN accelerators [33, 34]. CiMLoop is built on the existing and proven tools Timeloop [41] and Accelergy [42]. Performance is modeled statistically rather than cyclebased for speed, while accuracy is maintained by operand-dependent simulation. The simulator itself is validated against the existing NeuroSim tool [35].

CiMLoop is distributed as a Docker container with a custom API interface to preserve the overall framework's modularity. We employ this interface to dispatch computation tasks to CiMLoop and retrieve results efficiently without introducing Docker-specific dependencies into the core simulation environment. This design choice facilitates the seamless replacement or addition of alternative compute simulators. Future work can easily integrate simulators for traditional CPU/GPU-based processing or systolic arrays [38] using our example implementation.

#### B. Communication Simulation

Accurate communication simulation is a key component in modeling the NoI and the associated data movement. As shown in Section V, communication time contributes significantly to overall execution time. Therefore, inaccurate modeling of the inter-chiplet communication greatly impacts overall accuracy. Moreover, accurate time progression cannot be modeled if inter-chiplet communication overhead is neglected or a lumped communication model decoupled from the DNN model layer computation is used. Since power and thermal analysis requires time-based metrics, co-simulating data movement with computation is required.

A broad range of communication simulators have been proposed to date [15, 16, 40, 43, 44]. The selected simulator must have certain functionality to simulate a chiplet-based system. This includes the ability to simulate large systems (hundreds of

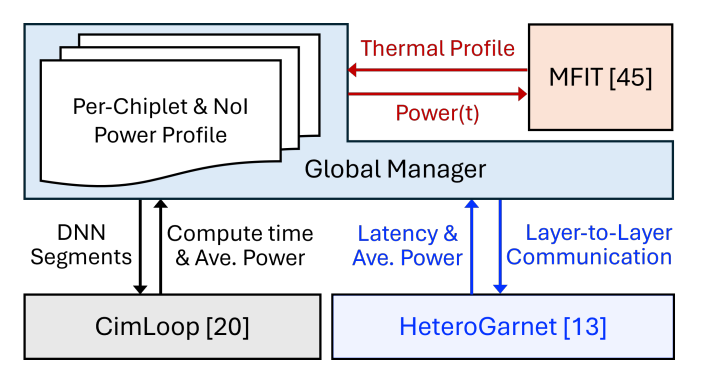


Fig. 5: The illustration of our concrete implementation and interface with thermal simulations.

chiplets), non-homogeneous links and clock domains, custom network topologies, and support for emerging interconnect standards such as UCIe [45]. We considered the alternatives listed in Table II and selected HeteroGarnet since it satisfies these requirements [15]. It was developed as a modification of the existing Garnet simulator, which was created for gem5 [13]. Unlike the event-based CiMLoop simulator, which was selected for computation simulation, HeteroGarnet is a cycle-accurate simulator. As the computations of each chiplet are independent from other computations, individual event-based compute simulation does not accumulate additional modeling error. In strong contrast, layer-to-layer communications contend for shared networking resources. Hence, their detailed cycle-accurate simulation is critical for capturing the interaction of different DNN models executing in parallel.

To integrate HeteroGarnet with the CHIPSIM framework, we further modified it with a more user-friendly method of topology description, making it simpler to create custom topologies in the network simulator itself, along with tracking for detailed simulation metrics associated with the network traffic injected by each source.

TABLE II: NoC simulator feature comparison.

NoC Simulator	Power Estimation	Custom Topology	UCIe Support	2.5D/3D Mixed	Hetero. Links
Booksim v2.0 [16]	N*	Y	Y	N	N
TOPAZ [44]	Y	Limited	N	N	N
Nostrum [43]	N	Limited	N	N	N
HeteroGarnet [15]	Y	Y	Y	Y	Y

## C. Power Analysis and Thermal Simulation

Thermal modeling and management of chiplet-based systems is crucial to preventing both thermal bottlenecks and potential damage to the system. Thermal simulation requires two primary inputs: a description of the physical system and a power profile over time for the chiplets.

Figure 5 shows the flow of power and thermal data in our concrete implementation of the proposed framework. The Global Manager takes the workload and system configuration defined by the user as input. It then executes the simulation, following the process described in Section III. As the simulation progresses, it stores the power consumption of each compute and communication operation, *along with when these operations took place and which chiplets completed the* 

*operation.* Using this information, the simulator constructs a time-based power profile for every chiplet in the system. This power profile is exported to the thermal model, shown on the right of Figure 5.

A wide range of thermal simulation tools have been proposed previously for both traditional monolithic chips and emerging chiplet-based systems [46–49]. In this work, we use the MFIT framework [49] to analyze thermal behavior due to its accuracy, efficiency, and flexible grid resolution. MFIT supports variable spatial granularity across layers. We employ a 2×2 thermal grid per chiplet in the active layer to capture intra-chiplet temperature variations, while using coarser grids (e.g., 10×10 nodes) in passive layers such as the interposer and heat spreader. This hierarchical modeling approach enables both localized hotspot analysis and efficient simulation of system-wide heat dissipation. After receiving the power profile and taking the system configuration as input, we construct the thermal profile of the system over time, as shown in Section V-D.

## V. EXPERIMENTAL EVALUATIONS

### A. Experimental Setup

**HW Configuration:** All experiments are evaluated on a  $10 \times 10$  chiplet system implemented on a 2.5D silicon interposer [18, 50]. The chiplets are configured using parameters from recent work [34]. The inter-chiplet NoI uses X-Y routing. In Sections V-B and V-D, chiplets are interconnected using a mesh NoI topology as in [23, 29]. Section V-C presents evaluations with alternate NoI topologies and chiplet compositions to demonstrate flexibility. The chiplet composition and interconnect topology of each evaluation is shown in the left two columns of Table III.

**Target DNN Models and Workload:** The driver workload consists of four common DNN models: AlexNet [51], ResNet18, ResNet34, and ResNet50 [52]. These models are selected as they provide a range of memory and processing requirements, where some layers require more than one chiplet.

Each simulated workload includes 50 DNN models, uniformly sampled at random from the four DNN types described earlier. The injection rate is set 1, meaning a DNN model is loaded into the model queue on each cycle. This high injection rate maximizes the system utilization. An age-aware scheduling policy is implemented to mitigate head-of-line blocking. If a model is too large to be mapped, the arbitration policy will skip the model and attempt to map the next model instead. The arbitration policy will prioritize oldest DNN models first, however, if a model passes an age threshold, it becomes non-skipable, and will block all younger models from mapping. Once launched, each model executes multiple backto-back inferences before being unmapped from the system, as explained in each section. The models included in each evaluation and the number of inferences swept are shown in the right two columns of Table III

**Simulation Parameters:** To balance simulation fidelity and runtime, CHIPSIM uses a configurable time step of  $1\mu$ s during co-simulation. This granularity was selected based on typical execution durations of DNN layer compute and communication phases, which range from several microseconds to

TABLE III: Evaluation configuration comparison.

Evaluation	Chiplet Composition	Interconn. Topol.	Models	# Inf. Swept
Non-pipelined Comparison	Homog. [34]	Mesh [23, 29]	AlexNet ResNets	10
Pipelined Comparison	Homog. [34]	Mesh [23, 29]	AlexNet ResNets	1, 3, 5 10, 20
Heterog. Comparison	Heterog. [33, 34]	Mesh [23, 29]	AlexNet ResNets	1, 3, 5 10, 20
Floret [18] Comparison	Homog. [34]	Floret [18]	AlexNet ResNets	1, 3, 5 10, 20
Transformer Evaluation	Homog. [34]	Mesh [23, 29]	ViT-B	1, 2, 5 10, 20

hundreds of microseconds in our setup. We validated that a smaller time step does not further improve the simulation results. A warm-up and cool-down time are applied to each simulation, during which simulation statistics are not collected. Both warm-up and cool-down times are set to 1 ms.

**Model to System Mapping:** To map DNN layers to the chiplet-based system, we use a nearest-neighbor mapping strategy inspired by Simba [29]. This mapper ensures that consecutive layers are mapped to spatially close chiplets, minimizing communication overhead.

Baseline Comparisons: We consider two baseline approaches for comparison to the CHIPSIM simulation framework. First, we consider the network-only approach utilized in NoI exploration works [17, 18]. In this baseline, only the network is simulated, and the compute simulation is omitted. We refer to this baseline as "Comm. Only". Second, we consider the approach implemented in SIAM, HISIM, and other more comprehensive works [23, 24]. We refer to this baseline as "Comm. + Compute". In this baseline approach, compute and communication are decoupled and simulated for each layer of each DNN model individually. In both baselines, only a single model is present in the system at a time during simulation. The same nearest-neighbor mapper that is utilized in CHIPSIM is used to map models for simulation using the baseline methods.

## B. Performance Comparisons vs Baseline Approaches

This section presents results using a mesh NoI and homogeneous chiplets with non-pipelined and pipelined operation.

1) Non-pipelined Operation: In this mode, there may be multiple DNN model instances that cause contention in the NoI, but layers of a given DNN model are executed one at a time without pipelining. This design choice does not fully exploit the system and leads to low utilization, but it can be preferred to simplify the hardware and software designs. Once launched, each model performs 10 back-to-back inferences before leaving the system.

Table IV compares the accuracy of the two baseline methods in predicting end-to-end inference latency against CHIPSIM. The *Comm. Only* baseline underestimates the latency by 22% (for ResNet50) to 74% (for ResNet18). These errors result from (1) the lack of compute simulation and (2) network traffic contention modeling in communication simulation.

The modeling error decreases by accounting for communication in the *Comm. + Compute* baseline, as expected. The

TABLE IV: Impact of co-simulation relative to baseline approaches for non-pipelined operation.

DNN Model	Percent Inaccuracy			
	Comm. Only	Comm. + Compute		
ResNet18	74%	8%		
ResNet34	70%	11%		
ResNet50	22%	9%		
AlexNet	33%	24%		

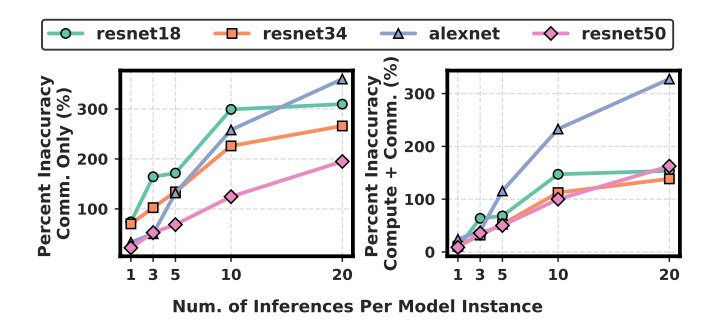


Fig. 6: The baseline approaches significantly underestimate the end-to-end inference time as the number of inferences per model (hence utilization) increases.

largest error occurs for AlexNet at 24%, while the smallest error occurs for ResNet18 at 8%. These results show that for non-pipelined operation, disaggregated *Comm. + Compute* simulation is a reasonable approximation of when the DNN model layers are non-pipelined. However, this inaccuracy increases dramatically with pipelining, as discussed next.

2) **Pipelined Operation**: A more optimized implementation pipelines the layers of each DNN model. Once a chiplet completes processing a layer and sends out the activations, it immediately starts the next inference round with the new input, while another chiplet processes its output. Hence, multiple layers of a given DNN model run in parallel.

Figure 6 compares the end-to-end inference latencies reported by CHIPSIM and baseline approaches as a function of inferences per DNN model. When the DNN models leave the system after only one inference, they do not exploit pipelining and operate like the non-pipelining case. The number of inferences repeated per model instance increases the number of parallel inferences, i.e., pipelining, and utilization. Hence, this experiment enables analyzing the accuracy benefits of CHIPSIM as a function of system utilization.

Aligned with the non-pipelined results, the *Comm. Only* baseline has significant inaccuracy, even with one or few inferences per model, since it fails to account for computation and network contention. The inaccuracy increases with the number of inferences per model instance. The error starts to saturate at 20 inferences, where AlexNet exceeds 340% latency inaccuracy and other models show 200-300% error, as the system reaches maximum utilization. Even at one inference per model instance, where pipelining is effectively disabled, ResNet18 and 34 show 74% and 69% error, respectively, while ResNet50 and AlexNet show lower error at 22% and 33% error, respectively.

The Comm. + Compute baseline exhibits a similar trend,

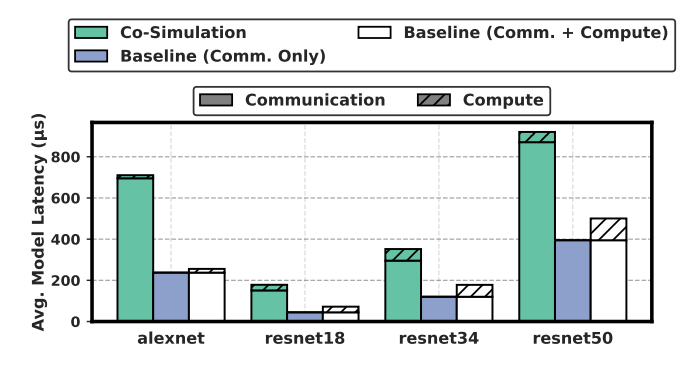


Fig. 7: Pipelined performance comparisons with 10 inferences per model.

though with lower underestimation. Again, the error starts saturating at the final data point of 20 inferences/model instance as more parallelism no longer increases the utilization. AlexNet experiences up to 320% modeling error, while the errors of the ResNet models range from 100% to 200%. There is a smaller (less than 30%) difference between using the baseline approach or co-simulation with a single inference for each model (effectively no pipelining), aligned with previous results.

Figure 7 plots the average compute and communication times for each model to analyze the root cause of the underestimation. Since multiple layers of each DNN model run in parallel with pipelining, large inter-chiplet communication volume and NoI utilizations lead to higher traffic contention and communication time. In these simulations, the communication time dominates the total inference time for this particular hardware configuration, since the selected chiplets have fast processing speeds. *Comm. Only* or *Comm. + Compute* baselines are inaccurate even under this condition since the proposed cosimulation approach is required to capture the network traffic timing and contention. The next section adds slower chiplets to the system to analyze scenarios where computation takes up a larger portion of the total processing time.

### C. Demonstrations with Different NoIs and Chiplet Types

1) Heterogeneous Chiplets: CHIPSIM supports systems composed of heterogeneous chiplets. To demonstrate this ability, we modify the original homogeneous 100 chiplet system to create a system with 50 chiplets of the original type and 50 of a different type based on a separate IMC work [33], with pipelining enabled. The chiplets are laid out in an alternating pattern, such that each chiplet is neighbored by chiplets of the other type.

The computation time increases significantly, reaching 42% of the total execution time for Resnet18, 44% for Resnet34, and 54% for Resnet50.

Table V compares the percent inaccuracy in results generated using the *Comm.* + *Compute* baseline as compared to CHIPSIM results. We exclude the *Comm. Only* baseline due to its previously demonstrated inaccuracy. The baseline method exhibits substantial inaccuracy in simulating this heterogeneous system. Again, the minimum error occurs with one inference per model instance, with a minimum error of

9% for AlexNet and a maximum error of 146% for ResNet18. As before, error increases substantially with the number of inferences. Maximum error occurs at the maximum number of inferences per model instance, with ResNet18 showing the largest inaccuracy of the baseline method at 632%, while ResNet50 shows the smallest at 233%.

TABLE V: Percent inaccuracy relative to baseline latency across inference counts using a heterogeneous system.

Num. of Inferences	Percent Inaccuracy				
	ResNet18	ResNet34	ResNet50	AlexNet	
1	146%	52%	49%	9%	
3	310%	113%	69%	39%	
5	353%	211%	81%	107%	
10	407%	250%	155%	224%	
20	632%	423%	233%	337%	

2) Alternate Topologies: Our co-simulation framework supports arbitrary NoI topologies beyond the mesh topology used in the previous section. We demonstrate this capability using the recently proposed Floret topology on the same 100-chiplet system [18], which is designed to optimize DNN execution by aligning the NoI structure with DNN data flows. Workloads and system configurations remain identical, and pipelining is enabled.

Table VI summarizes the percentage error of the *Comm. + Compute* baseline only relative to CHIPSIM since the *Comm. Only* baseline is shown to be inferior. As observed with the mesh topology, the baseline error grows with increasing inferences per model. At one inference per model, where the pipelining effects are negligible, the maximum error is 17% (AlexNet). The error increases with more inference per model (hence, utilization). At 20 inferences per model, errors escalate dramatically, reaching 120% for ResNet34 and 337% for AlexNet.

### D. Power and Thermal Analysis

In addition to performance results, each simulation run with our co-simulation framework generates power consumption profiles over time for every chiplet in the system. Figure 8 presents the power profiles of three representative chiplets executing a full workload (upper plot) along with the total system power consumption (lower plot). The per-chiplet profiles clearly show transient power spikes, such as those observed in chiplets 1 and 51. Our implementation captures power at  $1\mu s$  granularity, enabling accurate modeling of short-lived power fluctuations that would be missed with coarser methods.

The lower plot of Figure 8 shows the total system power. Smaller models, which require fewer chiplet resources, are mapped and execute earlier in the simulation as they are less likely to be blocked from mapping, while larger models, which require more memory, execute later in the simulation as more memory becomes free. This behavior is accurately reflected in the power consumption profile, which shows a significant power spike early in the simulation. It is followed by rapidly fluctuating power levels before power stabilizes at around the 50 W range.

TABLE VI: Percent inaccuracy relative to baseline latency across inference counts using the Floret NoI.

Num. of Inferences	Percent Inaccuracy				
	ResNet18	ResNet34	ResNet50	AlexNet	
1	14%	13%	9%	17%	
3	56%	42%	30%	24%	
5	68%	53%	49%	131%	
10	94%	102%	103%	235%	
20	126%	120%	128%	337%	

These detailed power traces are then used as inputs to our integrated fast thermal model, as described in Section IV-C. The thermal model analyzes the transient temperature and steady-state thermal profile of each chiplet using this input. Illustrative thermal maps are shown in Figure 9, where darker colors show which chiplets reach higher temperatures. This heatmap allows the user to visualize hotspots within the chiplet-based system. The power-thermal analysis capability allows precise analysis of how workload execution affects chiplet temperatures, providing critical insights for thermal management and reliability assessment.

### E. Transformer Model Demonstration

The CHIPSIM framework is capable of simulating transformer models in addition to the previously demonstrated CNN models. To demonstrate this ability, we simulate the ViT-B/16 [53] model on the same system used to simulate CNN models in Section 5.b. This system has 100 chiplets of identical type with a mesh interconnect with the following modifications:

- The four corner chiplets are designated as I/O chiplets, responsible for hosting and distributing model weights.
- The system adopts weight-stationary in-memory compute (IMC): weights are loaded once at the beginning and reused across inferences.
- We simulate single-model execution with input pipelining, without concurrent model instances, due to the memory footprint of ViT-B/16.

Due to the weight storage requirements of a single Vit-B model, a single instance of the model is simulated without the parallel execution of any additional models. As with previous shown results, pipelining of inputs is enabled in this example.

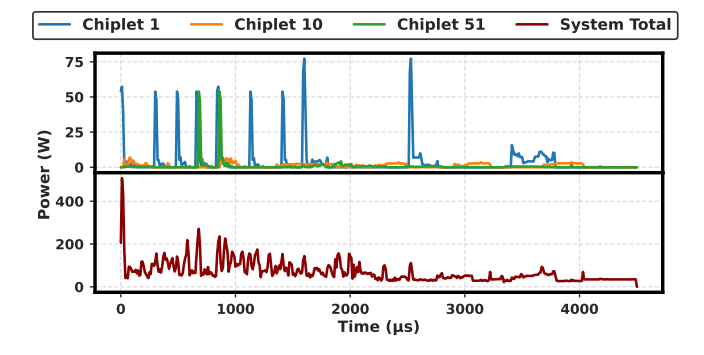


Fig. 8: Upper plot shows per-chiplet power over time of 3 selected chiplets. Lower plot shows System Total power over time.

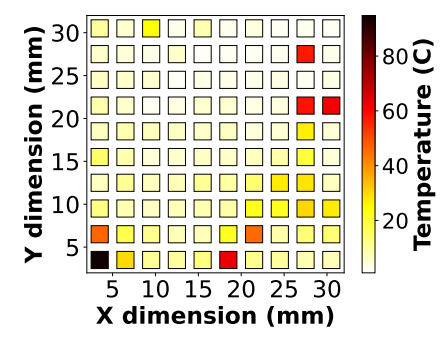


Fig. 9: Heatmap at the end of simulation.

Figure 10 shows the impact of increasing the number of inferences completed by the ViT-B model. The left subplot shows the difference between the results of CHIPSIM and the communication only baseline, while the right shows the difference between CHIPSIM and the compute + communication baseline. There is no difference at one inference per model since only a single model is running. The difference increases and reaches 25% at 20 inferences per model for the communication only baseline, and 24% for the compute + communication baseline. The smaller difference in results between the baseline and CHIPSIM results for this experiment is driven by two factors. First, for a single inference, weight loading time is dominant, taking about three times longer than the execution of the model, and is accounted for in both the baseline and CHIPSIM results. The impact of this fixed overhead becomes relatively less as the number of inferences increases. At larger numbers of inferences, the difference between baseline and CHIPSIM results is driven by contention between pipelined inputs and parallel model execution. As no parallel models exist in this simulation, only pipelined input contention causes inaccuracy, explaining the relatively lower difference between CHIPSIM and baseline results. The relatively smaller difference between the communication only and compute + communication baseline is due to the dominance of communication latency during ViT-B execution, leading to a very small difference between these two baselines.

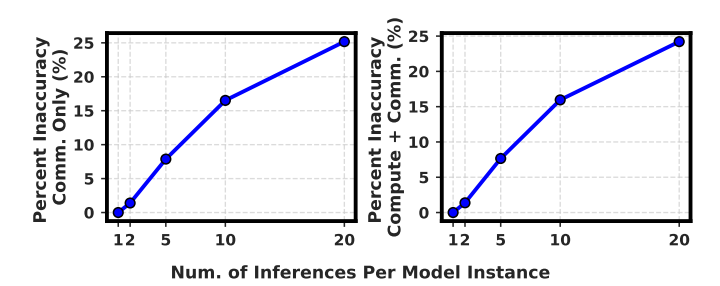


Fig. 10: Baseline vs CHIPSIM results for ViT-B execution.

# F. Hardware Validation

**Hardware Setup:** We further validate the proposed CHIPSIM framework against hardware measurements collected on an AMD Ryzen Threadripper PRO 7985WX (64 cores) platform [54]. This platform contains 8 CCD (compute complex

die) chiplets and 1 IOD (I/O die) responsible for chiplet-to-chiplet and DRAM communication. Each CCD contains 8 cores and connects to the IOD via Global Memory Inter-connect (GMI3) links, while the IOD interfaces with DDR5 memory. Notably, the GMI3 fabric provides asymmetric bandwidth per direction (32 B/cycle for read, 16 B/cycle for write at 1.733 GHz), corresponding to ~55 GB/s read and ~27.7 GB/s write per link.

DL Workload Modeling on Chiplet Platforms: DL workloads consist of interleaving computation within a layer/module (e.g., fully connected layer, attention block) and communication of the produced activation outputs. Computations are confined within a processing unit (like a chiplet), while communication is between chiplets and memory. To mimic execution of DL workloads on IMC platforms, we develope a macro-kernel workload that integrates load, compute, and store phases in a configurable loop. Our macro-kernels allow explicit compute and communication scheduling with parameters that control their duration. Each CCD in the AMD Ryzen Threadripper PRO 7985WX platform executes this workload independently, emulating multiple DNNs executing concurrently on different chiplets, similar to our IMC chiplet setup.

To simulate this system in CHIPSIM, we first implement the same topology present in the hardware system in HeteroGarnet by configuring heterogeneous links that match the measured read/write bandwidth of each CCD as well as the IOD-to-DDR interface. This setup allows us to capture inter-chiplet and memory communication. CiMLoop is replaced with an analytical compute model created from the FLOPs/sec measured for each chiplet while computing micro-kernel benchmarks. This approach ensures that the compute throughput in CHIPSIM faithfully reflects the actual platform characteristics. CHIPSIM provides a realistic co-simulation of parallel DL workloads on a chiplet-based CPU by integrating both the bandwidth-calibrated communication model and the analytically derived compute model.

Hardware Profiling: For ground-truth measurements, we first employ the LIKWID microkernel suite [55]. Load-store benchmarks exclude computation to isolate communication costs. Figures 11(a)(b) show single-CCD read and write bandwidth scaling with threads, saturating at  $\sim$ 49 GB/s and  $\sim$ 27 GB/s, respectively. These values achieve ~90% (read) and  $\sim$ 98% (write) of the theoretical GMI3 peak. Figures 11(c)(d) report aggregate bandwidth across multiple CCDs, with all 8 threads per CCD enabled. Read bandwidth scales to  $\sim$ 270 GB/s, while write bandwidth saturates around 115 GB/s, demonstrating DDR congestion as more CCDs become active. These measurements approach the advertised DDR5 peak bandwidth of  $\sim$ 330 GB/s, reaching  $\sim$ 83% utilization. This close alignment confirms that our profiling captures the characteristics of the underlying platform and provides a reliable ground truth for evaluating ChipSim.

Validation of Chipsim Results: Three identical CNN workloads are executed on both the AMD Ryzen Threadripper PRO 7985WX platform and our simulator. For the first scenario, a single chiplet executes a single instance of AlexNet. The

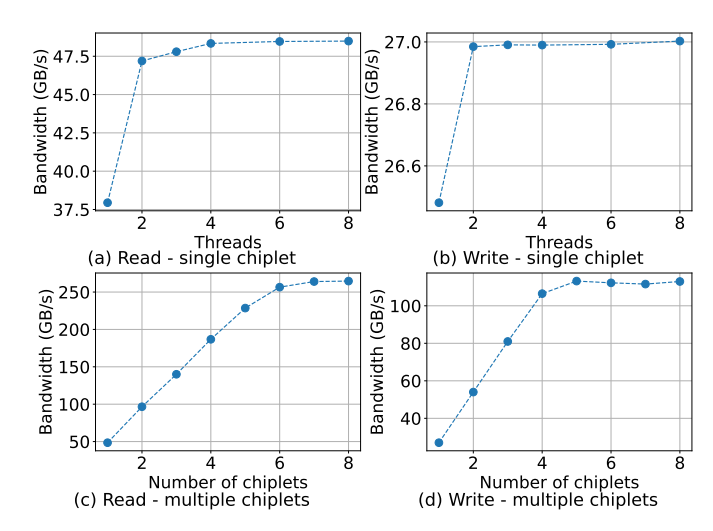


Fig. 11: Measured bandwidth results on the AMD Ryzen Threadripper PRO 7985WX platform. (a) Single-CCD read bandwidth as function of active threads. (b) Single-CCD write bandwidth as a function of active threads. (c) Aggregate read bandwidth as a function of active CCDs, each running 8 threads. (d) Aggregate write bandwidth as a function of active CCDs, each running 8 threads.

second scenario executes two instances of AlexNet on two different chiplets. Finally, the third scenario executes one instance of AlexNet, ResNet18, ResNet34, and ResNet50 each on four different chiplets. Table VII reports the percentage difference between measured and simulated times for each model. The third column shows the error in execution latency for each individual model, while the last column shows the average error across all models. CHIPSIM results align closely with hardware measurements, showing a maximum average error of only 2.51% for the four chiplet scenario and a minimum error of 0.75% for the two chiplet scenario. Permodel maximum error is less than 6%, seen when comparing results of simulating ResNet50. These results demonstrate that CHIPSIM not only enables design space exploration for new architectures but also provides highly accurate predictions against existing hardware platforms.

TABLE VII: Percent difference of CHIPSIM results as compared to hardware results.

Num. of Chiplets   Models		% Diff. from HW	Avg. % Diff.
One Chiplet	AlexNet	0.77%	0.77%
Two Chiplets	AlexNet (1)	0.64%	0.75%
	AlexNet (2)	0.86%	0.75%
Four Chiplets	AlexNet	1.29%	
	ResNet18	0.84%	2.51%
	ResNet34	2.19%	2.31%
	ResNet50	5.74%	

# G. Execution Time Analysis

Table VIII lists the average runtime per DNN model for each simulation approach. The CHIPSIM framework has an execution time of 12.6 minutes per model. In comparison, the Comm. + Compute baseline takes 12.2 minutes per model. The small increase in execution time shown by CHIPSIM is due to the additional overhead required for accurately tracking the state of the system, making mapping decisions, and coordinating the execution of component simulators. These results show that substantial accuracy improvement of CHIPSIM comes at a moderate increase in the execution time.

Our CHIPSIM implementation already performs cycle-accurate communication simulation using Hetero Garnet [15]. Further accuracy improvement can be achieved by making computation simulations also cycle-accurate. Since the most common choice, gem5 [13], cannot simulate the system considered in this work due to the use of IMC, we use another prior work that simulates DNN workloads on non-IMC systems using gem5 [56]. This prior work demonstrates that performing cycle-accurate simulation of DNN models in gem5 takes on the order of weeks. This massive execution time makes cycle-accurate computation-communication simulations infeasible for rapid evaluations, while CHIPSIM achieves speed, accuracy, and modularity through carefully optimized co-simulations.

TABLE VIII: Simulation runtime comparison across methods.

Simulation Method	Avg. Execution Time per Model
CHIPSIM (This Work)	12.6 min
Comm. + Compute Baseline	12.2 min
Cycle-Accurate (gem5)	Weeks [56]

## VI. CONCLUSION

In this work, we introduce CHIPSIM, a fast and accurate co-simulation framework for chiplet-based systems executing deep neural networks. By modeling computation and communication together with a coherent global timeline, CHIPSIM captures key effects like pipelining and network contention that are missed by traditional methods. Evaluations show that existing approaches can wrongly estimate latency by over 800% under realistic workloads. In contrast, CHIPSIM delivers high accuracy with fast runtime and supports detailed power and thermal analysis, making it a valuable tool for designing and optimizing chiplet-based systems.

# REFERENCES

- [1] Y. Sun, N. B. Agostini, S. Dong, and D. Kaeli, "Summarizing cpu and gpu design trends with product data," *arXiv preprint arXiv:1911.11313*, 2019.
- [2] J. A. Cunningham, "The use and evaluation of yield models in integrated circuit manufacturing," *IEEE Transactions on semiconductor manufacturing*, vol. 3, no. 2, pp. 60–71, 1990.
- [3] A. Graening *et al.*, "Cost-performance co-optimization for the chiplet era," in 2024 IEEE 26th Electronics Packaging Technology Conference (EPTC). IEEE, 2024, pp. 40–45.
- [4] S. Naffziger *et al.*, "Pioneering chiplet technology and design for the amd epyc<sup>TM</sup> and ryzen<sup>TM</sup> processor families: Industrial product," in *Proc. of ACM/IEEE ISCA*, 2021, pp. 57–70.

- [5] D. Stow, I. Akgun, R. Barnes, P. Gu, and Y. Xie, "Cost analysis and cost-driven ip reuse methodology for soc design based on 2.5d/3d integration," in *Proc. of IEEE/ACM ICCAD*, 2016, pp. 1–6.
- [6] H. Sharma, A. Kanani, J. R. Doppa, U. Y. Ogras, and P. P. Pande, "Hemu: Energy-efficient dnn inferencing via heterogeneous-multi-chiplet architectures," *IEEE Trans*actions on Computer-Aided Design of Integrated Circuits and Systems, 2025.
- [7] A. Kanani, L. Pfromm, H. Sharma, J. Doppa, P. Pande, and U. Ogras, "Thermos: Thermally-aware multiobjective scheduling of ai workloads on heterogeneous multi-chiplet pim architectures," ACM Transactions on Embedded Computing Systems, 2025.
- [8] I. Goldwasser, H. Petty, P. Desale, and K. Devleker, "NVIDIA GB200 NVL72 Delivers Trillion-Parameter LLM Training and Real-Time Inference," NVIDIA Technical Blog, 2024, accessed 29 June 2025. [Online]. Available: https://developer.nvidia.com/blog/ nvidia-gb200-nvl72-delivers-trillion-parameter-Ilm-training-and-real
- [9] Intel Corporation, "Agilex™ fpgas deliver a game-changing combination of flexibility and agility for the data-centric world," Intel Corporation, White Paper, Jan. 2024, describes chiplet integration using EMIB in Agilex FPGA products.
- [10] W. Gomes, S. Morgan, B. Phelps, T. Wilson, E. Hallnor, and et al., "Meteor lake and arrow lake: Intel next-gen 3d client architecture platform with foveros," in *Hot Chips 34 Symposium*, Aug. 2022, slides available from Hot Chips (IEEE Symposium).
- [11] National Institute Standards and of Technology "CHIPS (NIST), National Advanced Packaging Manufacturing Program (NAPMP)," https: //www.nist.gov/chips/research-development-programs/ national-advanced-packaging-manufacturing-program, 2025, accessed: 2025-06-28.
- [12] —, "Scalable Memory Architecture Program (SMAP)," https://natcast.org/assets/uploads/2025/05/SMAP-CFP-V1.1.pdf, 2025, 30-month initiative; Accessed: 2025-06-28.
- [13] J. Lowe-Power, A. M. Ahmad, A. Akram, M. Alian, R. Amslinger, M. Andreozzi, A. Armejach, N. Asmussen, B. Beckmann, S. Bharadwaj et al., "The gem5 simulator: Version 20.0+," arXiv preprint arXiv:2007.03152, 2020.
- [14] N. Binkert, B. Beckmann, G. Black, S. K. Reinhardt, A. Saidi, A. Basu, J. Hestness, D. R. Hower, T. Krishna, S. Sardashti et al., "The gem5 simulator," ACM SIGARCH computer architecture news, vol. 39, no. 2, pp. 1–7, 2011.
- [15] S. Bharadwaj, J. Yin, B. Beckmann, and T. Krishna, "Kite: A family of heterogeneous interposer topologies enabled via accurate interconnect modeling," in 2020 57th ACM/IEEE Design Automation Conference (DAC). IEEE, 2020, pp. 1–6.
- [16] N. Jiang, D. U. Becker, G. Michelogiannakis, J. Balfour, B. Towles, D. E. Shaw, J. Kim, and W. J. Dally, "A detailed and flexible cycle-accurate network-on-chip simulator," in 2013 IEEE international symposium on

- performance analysis of systems and software (ISPASS). IEEE, 2013, pp. 86–96.
- [17] P. Iff, M. Besta, M. Cavalcante, T. Fischer, L. Benini, and T. Hoefler, "Hexamesh: Scaling to hundreds of chiplets with an optimized chiplet arrangement," in 2023 60th ACM/IEEE Design Automation Conference (DAC). IEEE, 2023, pp. 1–6.
- [18] H. Sharma et al., "Florets for chiplets: Data flow-aware high-performance and energy-efficient network-on-interposer for cnn inference tasks," ACM Transactions on Embedded Computing Systems, vol. 22, no. 5s, pp. 1–21, 2023.
- [19] H. Sharma, S. K. Mandal, J. R. Doppa, U. Y. Ogras, and P. P. Pande, "Swap: A server-scale communicationaware chiplet-based manycore pim accelerator," *IEEE Transactions on Computer-Aided Design of Integrated Circuits and Systems*, vol. 41, no. 11, pp. 4145–4156, 2022.
- [20] P. Iff, B. Bruggmann, M. Besta, L. Benini, and T. Hoefler, "Rapidchiplet: A toolchain for rapid design space exploration of chiplet architectures," arXiv preprint arXiv:2311.06081, 2023.
- [21] F. Li, Y. Wang, Y. Cheng, Y. Wang, Y. Han, H. Li, and X. Li, "Gia: A reusable general interposer architecture for agile chiplet integration," in *Proceedings of the 41st IEEE/ACM International Conference on Computer-Aided Design*, 2022, pp. 1–9.
- [22] T. Andrulis, J. S. Emer, and V. Sze, "Cimloop: A flexible, accurate, and fast compute-in-memory modeling tool," in 2024 IEEE International Symposium on Performance Analysis of Systems and Software (ISPASS). IEEE, 2024, pp. 10–23.
- [23] G. Krishnan, S. K. Mandal, M. Pannala, C. Chakrabarti, J.-S. Seo, U. Y. Ogras, and Y. Cao, "Siam: Chipletbased scalable in-memory acceleration with mesh for deep neural networks," ACM Transactions on Embedded Computing Systems (TECS), vol. 20, no. 5s, pp. 1–24, 2021.
- [24] Z. Wang, P. S. Nalla, J. Sun, A. A. Goksoy, S. K. Mandal, J.-s. Seo, V. A. Chhabria, J. Zhang, C. Chakrabarti, U. Y. Ogras et al., "Hisim: Analytical performance modeling and design space exploration of 2.5 d/3d integration for ai computing," *IEEE Transactions on Computer-Aided Design of Integrated Circuits and Systems*, 2025.
- [25] G. Krishnan, A. A. Goksoy, S. K. Mandal, Z. Wang, C. Chakrabarti, J.-s. Seo, U. Y. Ogras, and Y. Cao, "Biglittle chiplets for in-memory acceleration of dnns: A scalable heterogeneous architecture," in *Proceedings of the* 41st IEEE/ACM International Conference on Computer-Aided Design, 2022, pp. 1–9.
- [26] H. Sharma, P. Dhingra, J. Doppa, U. Ogras, and P. P. Pande, "A heterogeneous chiplet architecture for accelerating end-to-end transformer models," *ACM Transactions on Design Automation of Electronic Systems*, vol. 30, no. 3, pp. 1–24, 2025.
- [27] A. Smith, G. H. Loh, M. J. Schulte, M. Ignatowski, S. Naffziger, M. Mantor, M. F. N. Kalyanasundharam, V. Alla, N. Malaya, J. L. Greathouse *et al.*, "Realizing the

- amd exascale heterogeneous processor vision: industry product," in 2024 ACM/IEEE 51st Annual International Symposium on Computer Architecture (ISCA). IEEE, 2024, pp. 876–889.
- [28] A. Jaiswal, K. S. Shahana, S. Ravichandran, K. Adarsh, H. B. Bhat, B. K. Joardar, and S. K. Mandal, "Halo: Communication-aware heterogeneous 2.5 d system for energy-efficient llm execution at edge," *IEEE Journal on Emerging and Selected Topics in Circuits and Systems*, 2024.
- [29] Y. S. Shao, J. Clemons, R. Venkatesan, B. Zimmer, M. Fojtik, N. Jiang, B. Keller, A. Klinefelter, N. Pinckney, P. Raina et al., "Simba: Scaling deep-learning inference with multi-chip-module-based architecture," in Proceedings of the 52nd annual IEEE/ACM international symposium on microarchitecture, 2019, pp. 14–27.
- [30] L. Song, X. Qian, H. Li, and Y. Chen, "Pipelayer: A pipelined reram-based accelerator for deep learning," in 2017 IEEE international symposium on high performance computer architecture (HPCA). IEEE, 2017, pp. 541–552.
- [31] M. Odema, L. Chen, H. Kwon, and M. A. Al Faruque, "Scar: Scheduling multi-model ai workloads on heterogeneous multi-chiplet module accelerators," in 2024 57th IEEE/ACM International Symposium on Microarchitecture (MICRO). IEEE, 2024, pp. 565–579.
- [32] A. Kannan, N. E. Jerger, and G. H. Loh, "Enabling interposer-based disintegration of multi-core processors," in *Proceedings of the 48th international symposium on Microarchitecture*, 2015, pp. 546–558.
- [33] T. Andrulis, J. S. Emer, and V. Sze, "Raella: Reforming the arithmetic for efficient, low-resolution, and low-loss analog pim: No retraining required!" in *Proceedings of the 50th Annual International Symposium on Computer Architecture*, 2023, pp. 1–16.
- [34] W. Wan, R. Kubendran, C. Schaefer, S. B. Eryilmaz, W. Zhang, D. Wu, S. Deiss, P. Raina, H. Qian, B. Gao et al., "A compute-in-memory chip based on resistive random-access memory," *Nature*, vol. 608, no. 7923, pp. 504–512, 2022.
- [35] X. Peng, S. Huang, Y. Luo, X. Sun, and S. Yu, "Dnn+neurosim: An end-to-end benchmarking framework for compute-in-memory accelerators with versatile device technologies," in 2019 IEEE international electron devices meeting (IEDM). IEEE, 2019, pp. 32–5.
- [36] H. Li, J. Li, and A. Kaufmann, "Simbricks: end-to-end network system evaluation with modular simulation," in *Proceedings of the ACM SIGCOMM 2022 Conference*, 2022, pp. 380–396.
- [37] A. F. Rodrigues, K. S. Hemmert, B. W. Barrett, C. Kersey, R. Oldfield, M. Weston, R. Risen, J. Cook, P. Rosenfeld, E. Cooper-Balis et al., "The structural simulation toolkit," ACM SIGMETRICS Performance Evaluation Review, vol. 38, no. 4, pp. 37–42, 2011.
- [38] A. Samajdar, Y. Zhu, P. Whatmough, M. Mattina, and T. Krishna, "Scale-sim: Systolic cnn accelerator simulator," *arXiv preprint arXiv:1811.02883*, 2018.
- [39] Y. Feng, Y. Wei, D. Xiang, and K. Ma, "Evaluating

- chiplet-based {Large-Scale} interconnection networks via {Cycle-Accurate}{Packet-Parallel} simulation," in 2024 USENIX Annual Technical Conference (USENIX ATC 24), 2024, pp. 731–747.
- [40] V. Catania, A. Mineo, S. Monteleone, M. Palesi, and D. Patti, "Noxim: An open, extensible and cycle-accurate network on chip simulator," in 2015 IEEE 26th international conference on application-specific systems, architectures and processors (ASAP). IEEE, 2015, pp. 162–163.
- [41] A. Parashar, P. Raina, Y. S. Shao, Y.-H. Chen, V. A. Ying, A. Mukkara, R. Venkatesan, B. Khailany, S. W. Keckler, and J. Emer, "Timeloop: A systematic approach to dnn accelerator evaluation," in 2019 IEEE international symposium on performance analysis of systems and software (ISPASS). IEEE, 2019, pp. 304–315.
- [42] Y. N. Wu, J. S. Emer, and V. Sze, "Accelergy: An architecture-level energy estimation methodology for accelerator designs," in 2019 IEEE/ACM International Conference on Computer-Aided Design (ICCAD). IEEE, 2019, pp. 1–8.
- [43] M. Millberg, E. Nilsson, R. Thid, S. Kumar, and A. Jantsch, "The nostrum backbone-a communication protocol stack for networks on chip," in *17th International Conference on VLSI Design. Proceedings*. IEEE, 2004, pp. 693–696.
- [44] P. Abad, P. Prieto, L. G. Menezo, V. Puente, J.-Á. Gregorio et al., "Topaz: An open-source interconnection network simulator for chip multiprocessors and supercomputers," in 2012 IEEE/ACM Sixth International Symposium on Networks-on-Chip. IEEE, 2012, pp. 99–106.
- [45] D. D. Sharma, G. Pasdast, Z. Qian, and K. Aygun, "Universal chiplet interconnect express (ucie): An open industry standard for innovations with chiplets at package level," *IEEE Transactions on Components, Packaging* and Manufacturing Technology, vol. 12, no. 9, pp. 1423– 1431, 2022.
- [46] R. Zhang, M. R. Stan, and K. Skadron, "Hotspot 6.0: Validation, acceleration and extension," *University of Virginia, Tech. Rep*, 2015.
- [47] A. Sridhar, A. Vincenzi, M. Ruggiero, T. Brunschwiler, and D. Atienza, "3d-ice: Fast compact transient thermal modeling for 3d ics with inter-tier liquid cooling," in 2010 IEEE/ACM International Conference on Computer-Aided Design (ICCAD). IEEE, 2010, pp. 463–470.
- [48] Z. Yuan, P. Shukla, S. Chetoui, S. Nemtzow, S. Reda, and A. K. Coskun, "Pact: An extensible parallel thermal simulator for emerging integration and cooling technologies," *IEEE Transactions on Computer-Aided Design of Integrated Circuits and Systems*, vol. 41, no. 4, pp. 1048–1061, 2021.
- [49] L. Pfromm, A. Kanani, H. Sharma, P. Solanki, E. Tervo, J. Park, J. Doppa, P. P. Pande, and U. Ogras, "Mfit: Multifidelity thermal modeling for 2.5 d and 3d multi-chiplet architectures," ACM Transactions on Design Automation of Electronic Systems, 2025.
- [50] P. Huang, C. Lu, W. Wei, C. Chiu, K. Ting, C. Hu,

- C. Tsai, S. Hou, W. Chiou, C. Wang *et al.*, "Wafer level system integration of the fifth generation cowos®-s with high performance si interposer at 2500 mm2," in 2021 IEEE 71st Electronic Components and Technology Conference (ECTC). IEEE, 2021, pp. 101–104.
- [51] A. Krizhevsky, I. Sutskever, and G. E. Hinton, "Imagenet classification with deep convolutional neural networks," *Communications of the ACM*, vol. 60, no. 6, pp. 84–90, 2017.
- [52] K. He, X. Zhang, S. Ren, and J. Sun, "Deep residual learning for image recognition," in *Proceedings of the IEEE conference on computer vision and pattern recognition*, 2016, pp. 770–778.
- [53] A. Dosovitskiy, L. Beyer, A. Kolesnikov, D. Weissenborn, X. Zhai, T. Unterthiner, M. Dehghani, M. Minderer, G. Heigold, S. Gelly *et al.*, "An image is worth 16x16 words: Transformers for image recognition at scale," *arXiv preprint arXiv:2010.11929*, 2020.
- [54] Advanced Micro Devices, Inc., "Ryzen threadripper pro 7000 wx-series (datasheet/brief)," 2023, includes model 7985WX specifications. [Online]. Available: https://www.amd.com/content/dam/amd/ en/documents/products/processors/ryzen-threadripper/ threadripper-pro-design-aec.pdf
- [55] J. Treibig, G. Hager, and G. Wellein, "Likwid: A lightweight performance-oriented tool suite for x86 multicore environments," in 2010 39th international conference on parallel processing workshops. IEEE, 2010, pp. 207–216.
- [56] V. Ramadas, M. Poremba, B. Beckmann, and M. D. Sinclair, "Simulation support for fast and accurate large-scale gpgpu & accelerator workloads," in *Third Workshop on Open-Source Computer Architecture Research*, ser. OSCAR, 2024.



**Lukas Pfromm** (Student Member, IEEE) is currently pursuing the Ph.D. degree in Computer Engineering at University of Wisconsin Madison, Madison, WI, USA. His research interests include chiplet system performance modeling, thermal modeling, and thermal management.



Alish Kanani (Student Member, IEEE) is currently pursuing the Ph.D. degree in Computer Engineering at University of Wisconsin Madison, Madison, WI, USA. His research interests include runtime thermal management and co-optimized system design.



Harsh Sharma (Graduate Student Member, IEEE) is currently pursuing the Ph.D. degree in Computer Engineering at Washington State University, Pullman, WA, USA. His research interests include heterogenous integration, and ML for computer-aided design.



Janardhan Rao Doppa (Senior Member, IEEE) received the Ph.D. degree in computer science from Oregon State University, Corvallis, OR, USA, in 2014. He is the Huie-Rogers Endowed Chair Associate Professor in Computer Science at Washington State University, Pullman, WA, USA.



Partha Pratim Pande (Fellow, IEEE) received the Ph.D. degree in electrical and computer engineering from the University of British Columbia, Vancouver, BC, Canada, in 2005. He is a professor and a holder of the Boeing Centennial Chair of Computer Engineering with the School of EECS, Washington State University, Pullman, WA, USA.



**Umit Y. Ogras** (Fellow, IEEE) received the Ph.D. degree from Carnegie Mellon University, Pittsburgh, PA, USA, in 2007. He is currently an Associate Professor with the Department of ECE at University of Wisconsin–Madison, Madison, WI, USA.